ELSEVIER

Polymer 43 (2002) 3311–3321

polymer

www.elsevier.com/locate/polymer

Morphology development in immiscible polymer blends during crystallization of the dispersed phase under shear flow

Y. Deyrail, R. Fulchiron, P. Cassagnau*

Laboratoire des Matériaux Plastiques et Biomatériaux, Université Claude Bernard, Lyon 1, 43 Blvd du 11 Novembre 1918, UMR 5627 Bat ISTIL, 69622 Villeurbanne Cedex, France

Received 15 October 2001; received in revised form 29 January 2002; accepted 8 February 2002

Abstract

Crystallization under shear of dispersed polybutylene terephthalate (PBT) fibers in copolymer polyethylene–methyl acrylate matrix (EMA) was investigated using a hot optical shear device. Crystallization during isotherm and cooling process was studied. Static crystallization experiments were carried out for comprehension purpose. Differential scanning calorimetry (DSC) analysis was performed in order to predict the crystallization behavior of PBT. Shear enhancement of its crystallization was thus demonstrated from rheological experiments. Interfacial tension of EMA/PBT blend was experimentally measured using the hot optical shear device. Theoretical break-up times of PBT fibers were also calculated. Control of the morphology through shear rate and crystallization time balance was demonstrated. Static crystallization experiments show that decreasing crystallization time favor fibrillar morphology. Breaking up of fibers was brought to the fore during dynamic crystallization experiments due to heterogeneous development of the crystallization along the fiber. During the dynamic crystallization, rapid quenching enables fibrillar morphology. Long crystallization times associated with low shear rates allow nodular morphology.

Keywords: Shear; Morphology; Crystallization

1. Introduction

Morphology development in immiscible polymer blends has been extensively studied for the past two decades. Indeed, the properties of a polymer blend material depend strongly on the morphology developed during the different processing steps. The final morphology of the dispersed phase depends on the properties of the blend component as well as on the processing operations. For example, it is well known that the morphology of a polymer blend is determined by the type of flow (shear or elongation), interfacial tension, composition and viscoelasticity of the components. Furthermore, different types of morphologies such as nodular, laminar or fibrillar ones of the dispersed phase can be obtained. The deformation/elongation of the dispersed phase particles is generated during processes like extrusion. For instance, adequate processing conditions, leading to elongation, rather than the break-up of the dispersed phase drops are required to have fibrillar morphology.

The deformation/break-up of drops can be understood from the Taylor [1] and Grace [2] analysis. The drop deformation, its aspect ratio and its eventual break-up are controlled by two dimensionless parameters, namely the viscosity ratio of the dispersed phase and the matrix

$$p = \eta_d/\eta_m \quad (1)$$

and the capillary number

$$\mathrm{Ca} = \sigma R/\gamma_{12} \quad (2)$$

which represents the ratio between viscous stresses (shear or elongational), σ, that tend to deform the drops and interfacial stresses, γ_{12}/R, that resist to the deformation and tend to restore the initial shape of the drop, R being the drop radius and γ_{12} the interfacial tension. Grace's [2] experimental studies have shown that the two parameters are linked and the possibility for the drop to sustain deformation without breaking up is given by an empirical critical capillary number, Ca_{crit}, that has to be compared with the actual local capillary number. By increasing the capillary number, the drop deformation increases linearly with Ca. Above Ca_{crit}, the particles break-up into smaller droplets. Grace [2] and many subsequent authors [3–5] have shown that Ca_{crit} depends not only on p but also on the nature of flow. In shear field, viscous drops (dispersed in viscous matrix)

* Corresponding author.
E-mail address: cassagno@matplast.univ-lyon1.fr (P. Cassagnau).

0032-3861/02/$ - see front matter
PII: S0032-3861(02)00134-9

with $p > 4$ never break; they deform into fibers and then rotate in the flow field. In contrast, viscous drops subjected to an extensional flow field can break-up at any value of p, provided that $Ca > Ca_{crit}$.

However, the drop deformation and break-up are in a sense transient phenomena that require a specific time which must be defined. Similar to the capillary number, the time scale can be defined (for shear flow for instance) in a dimensionless form

$$t_{crit} = \frac{t_b \dot{\gamma}}{Ca} \tag{3}$$

where t_b is the break-up time under quiescent conditions via Rayleigh instabilities

$$t_b = \frac{2\eta_m R_0}{\gamma_{12}\Omega(\chi_m, p)} \ln\left(\frac{\alpha_r}{\alpha_i}\right) \tag{4}$$

where $\Omega(\chi_m, p)$ is a complex function of the viscosity ratio and the instability wavenumber, tabulated by Tomotika [6], α_i and α_r are the initial and break-up amplitude of the Rayleigh instability. D_0 represents the initial diameter of the thread. The drop can break only if $p < 4$ and $t > t_b$. However, this break-up mechanism is assumed to occur under quiescent conditions, when the flow is stopped or at low Deborah numbers D_b

$$D_b = \tau_d / t_r \tag{5}$$

τ_d being the relaxation time and t_r the residence time. During the extrusion process, this can occur in small pressure gradient zones or in long dies at low extrusion speed where D_b is very small. During flow, the main critical parameter is the ratio between the rate of the thread diameter reduction by Rayleigh instabilities and by flow (shear or extensional). This leads to a link between the break-up time and the rate of deformation (shear or extensional).

Nevertheless, the quenching time t_q, which is the time for freezing the morphology by crystallization or solidification of the dispersed phase, must be taken into account. Usually, the morphologies and/or the mechanical properties are observed at room temperature. Consequently, these properties depend not only on the deformation/elongation of the dispersed phase in melt state but also on the quenching processing conditions. This is particularly true for immiscible blends named organic composite systems for which the dispersed phase will crystallize or solidify in a melt viscoelastic matrix. For example, we reported in a previous work [7] that a new type of morphology can be obtained from a process which consists in crystallizing under shear or elongational flows a semi-crystalline polymer (or solidifying an amorphous polymer) dispersed in melt thermoplastic matrix.

One of the aims of the present work is to study the crystallization under shear flow of polybutylene terephthalate (PBT) particles dispersed in a melt matrix of ethylene and methyl acrylate copolymer. For this purpose, a hot optical shear device was used in order to visualize the influence of the different time parameters on the development of the blend morphology under shear flow.

2. Experimental part

2.1. Materials

Copolymer of ethylene–methyl acrylate was supplied in pellet form by AtoFina (EMA, 29% acrylate, MFI 03, M_n = 22 kg/mol, M_w = 94.3 kg/mol, density = 0.95 g/cm^3). Polybutylene terephtalate was supplied by Dupont in pellet form as well (PBT, Crastin S600, density = 1.31 g/cm^3) and has been dried under vacuum for one night at 80 °C. For rheological and observation purpose, EMA pellets were put into plate form under press at 200 °C. Then PBT pellets were ground into powder ($\phi \approx 100$ μm) so it can be dispersed in an EMA sandwich for shear experiment under microscope.

2.2. Rheological analysis

Frequency and time sweep experiments on molten samples were carried out on a Rheometrics SR5 stress controlled rheometer using both cone-plate ($\theta = 0.1$ rad, $\phi = 25$ mm) and parallel-plates geometry ($\phi = 25$ mm). In all cases, sample response linearity with respect to stress amplitude was verified and nitrogen gas was used to prevent thermal degradation. Zero shear viscosities of the components were measured at 250 °C (Table 1). At this temperature, PBT exhibits a Newtonian behavior on a large shear rate scale contrary to EMA that exhibits a pronounced shear thinning behavior above $\dot{\gamma} = 1\ s^{-1}$ (Fig. 1). Such behavior is exacerbated with decreasing the analysis temperature. However, in the temperature range used in this work ($T > 190$ °C), the rheological behavior of the EMA matrix is Newtonian.

2.3. DSC analysis

The thermal behavior of pure PBT was analyzed using Perkin–Elmer differential scanning calorimeter (model 7)

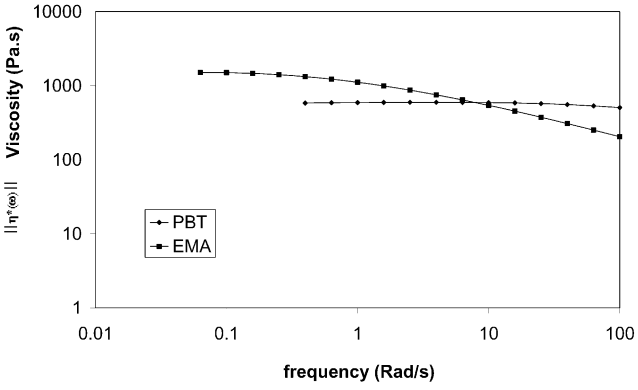

Fig. 1. Rheological behavior of pure PBT and pure EMA at 250 °C.

Table 1
General characteristics of the materials

Acronym	Polymer	T_m (°C)	T_g (°C)	η_0 (Pa s, 250 °C)
EMA	Copolymer ethylene–methyl acrylate		−30	1600
PBT	Polybutylene terephtalate	224	60	450

calibrated with indium and zinc. Experiments were performed under nitrogen atmosphere and weight of the samples were approximately 10 mg in order to obtain a significant signal. Heating and cooling ramp analyses as well as isothermal experiments have been done with various rates from 2 to 30 °C/min. These experiments aim at finding an appropriate crystallization time for the optical shear experiments. Indeed, we will deal later with breaking time of threads, generated from the sheared molten PBT particles, that has to be far longer than crystallization time. Isothermal experiments were carried out at several temperatures between 215 and 190 °C. Half times of crystallization were calculated and reported in Table 2. Cooling ramp tests were carried out so as to evaluate the crystallization time during cooling process. Different rates were used: 2, 10 and 30 °C/min, corresponding to those used with the optical shear device. Note that the crystallization temperature will vary with the cooling rate from 201 to 190 °C (at the start of the crystallization) and the crystallization times will be shorter than in isothermal conditions.

2.4. Optical shear experiments

Molten blends of EMA and PBT (PBT in very diluted conditions) were observed, in quiescent state or during shear, using a Leitz Orthoplan microscope (transmission) with 20× lens coupled with a Linkam CSS-450 high temperature stage. For contrast purpose during the crystallization, polarized light can be used. The sample was held in the gap between the two quartz windows (Fig. 2) and was sheared by rotating the bottom plate by a precision stepping motor, while the top plate remained stationary. So as to insure a complete cohesion between the EMA films and consequently that the dispersed PBT particles are completely imbedded, the gap between the windows is modified, using a stepping motor, to a value smaller than the thickness of the two EMA films. Such fitting is realized above 100 °C, when the viscosity of EMA is sufficiently low. Shear experiments were carried out at various shear rate from 0.17 to 3.4 s^{-1}. Such device allows us to study the behavior of EMA/PBT blends during a dynamic cooling process. A video camera was used to take pictures during the experiments. The shortest time between two shots is 4 s which enables us to follow rather continuously the dimensional evolution of the PBT drops or PBT threads. Most of the work was focused on the crystallization of PBT under shear flow. In order to understand the influence of shear rate and of crystallization time on the final morphology of the blend, several tests have been carried out.

Table 2
Half time of crystallization of pure PBT; isothermal experiments

Temperature (°C)	$t_{1/2}$ (s)
190	40
200	130
206	477
208	717
209	914
210	1140
215	3090

2.5. Determination of the interfacial tension by the drop retraction method

According to the work of Utracki [8], measurements of interfacial tension were carried out on a EMA/PBT blend. Using the Linkam device, a step deformation is imposed to a melt drop of PBT imbedded in molten EMA matrix. The relaxation process is then optically recorded until the drop returned from an ellipsoidal to an equilibrium spherical shape. Then, knowing the viscosity of both components, the interfacial tension can be inferred from the dimensional variations of the deformed drop as a function of the relaxation time. Such experiment is carried out on different

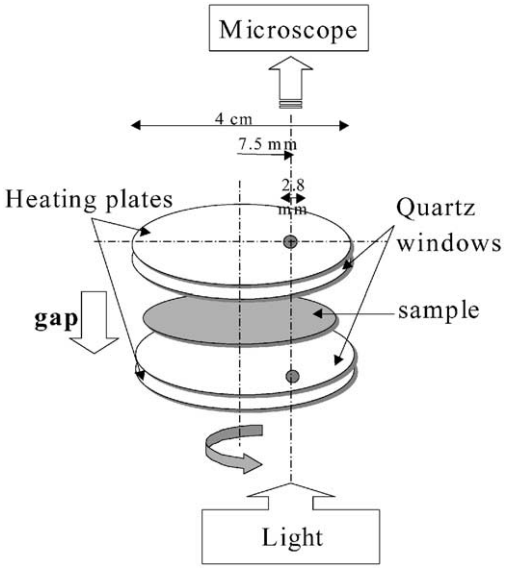

Fig. 2. Schematics of the Linkam shear device, showing the placement of the sample and the rotating and fixed windows. The scheme on the left shows the observation section which consist in the holes in the heating plates.

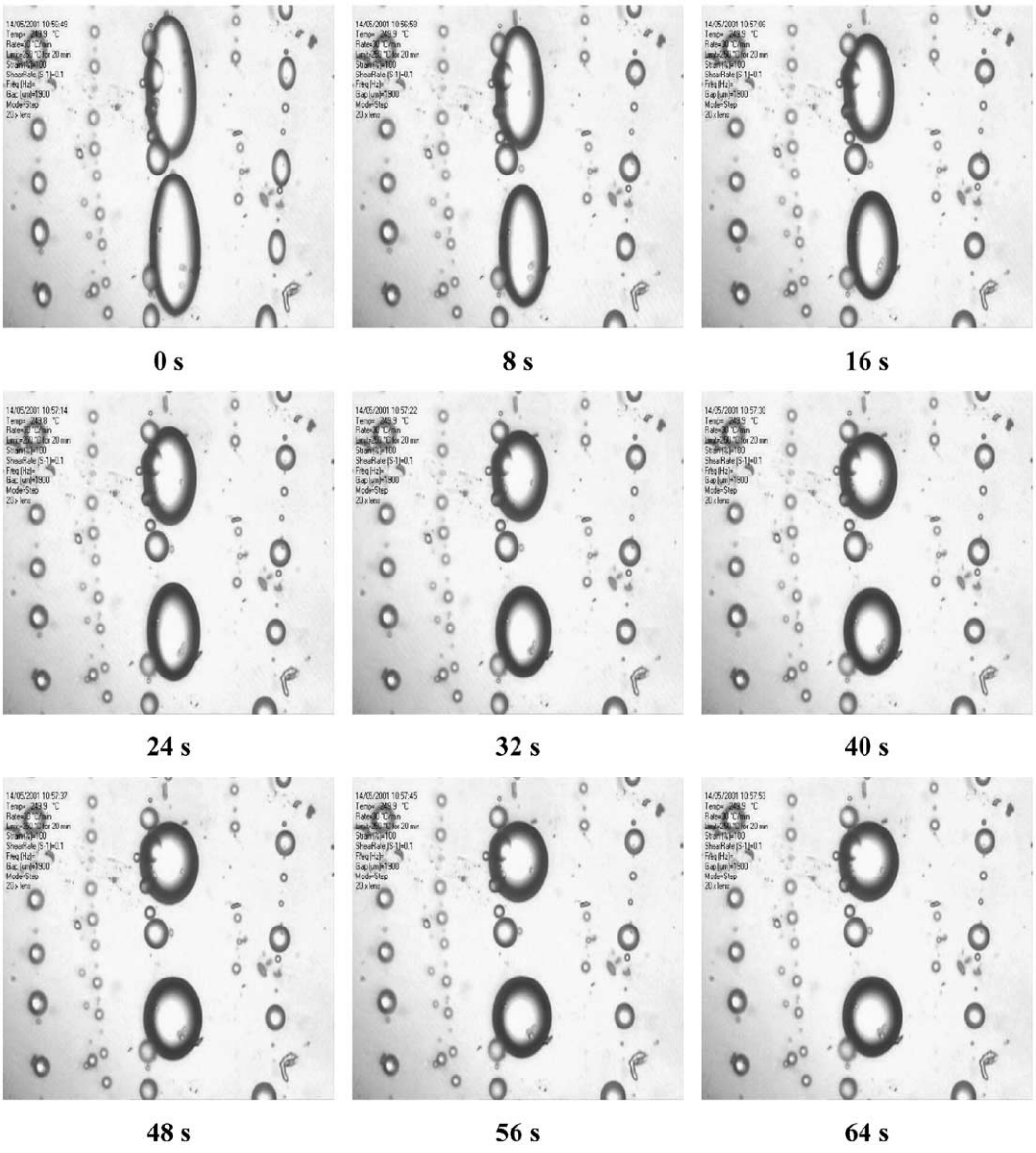

Fig. 3. Retraction of a PBT ellipsoidal droplet immersed in EMA matrix at 250 °C. The spherical particle diameter is $D_0 = 86$ μm; time of measurement is reported on each picture.

droplets so as to obtain reproducible values of interfacial tension. The various PBT droplets were obtained from fine PBT powder dispersed between two circular EMA films, the thickness of which is about 500 μm. In order to obtain well-defined spherical droplets, the dispersed particles were subjected to shear treatment for few seconds (30 s; steady shear 0.34 s^{-1}), giving rise to short filaments of PBT. The flow is then stopped and filaments are allowed to retract and to break into smaller domains. Such treatment enables us on the one hand to handle measurements on well-defined spherical PBT drops dispersed in EMA matrix, and on the other hand to reduce the initial particle size from 200 to 50–100 μm (average diameter). The so obtained spherical drop sustained several step-strains so as to be deformed into an ellipsoid of revolution and then optical measurements with the video camera coupled to the microscope were started. Typical pictures of the retraction of a deformed droplet are shown in Fig. 3.

Referring to Taylor's [1] theory, it is known that the recovery of a deformed viscous drop, immersed in a second fluid submitted to shear treatment, at small amplitude of deformation, is only driven by interfacial tension. Moreover, the rheological properties of the polymer do not change during the recovery process. Many reviews [9–10] deal with the determination of the interfacial tension. Bousmina et al. [11] sets out in detail calculations of the interfacial tension from a deformed drop retraction experiment. The calculation is based on the following expression of the deformation D

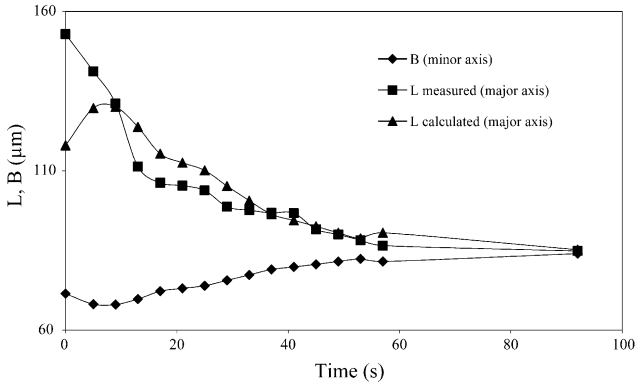

Fig. 4. Time evolution of the minor axis (B) and the major axis (L) for a PBT droplet immersed in an EMA matrix at 250 °C. The values of L were both measured and calculated for comparison. The diameter of the equilibrium spherical droplet is 84.4 μm.

towards the equilibrium shape of the droplet:

$$D = D_0 \exp\left\{-\frac{40(p+1)}{(2p+3)(19p+16)}\frac{\gamma_{12}}{\eta_m R_0}\right\}$$

$$= D_0 \exp\left\{-\frac{t}{\tau_d}\right\} = \frac{L-B}{L+B} \quad (6)$$

where D_0 is the deformability parameter at the initial time t_0, p is the viscosity ratio, L and B represent, respectively, the major and the minor axis of the ellipsoid and γ_{12} represents the interfacial tension. Knowing the relaxation time τ_d as:

$$\tau_d = \frac{\eta_{eq} R_0}{\gamma_{12}} \quad (7)$$

With the equivalent viscosity

$$\eta_{eq} = \frac{(2p+3)(19p+16)\eta_m}{40(p+1)} \quad (8)$$

where η_m is the zero shear viscosity of the matrix and R_0 is the initial drop radius.

From the appropriate curves (Figs. 4 and 5) and the corresponding linear fits, we have access to the value of the

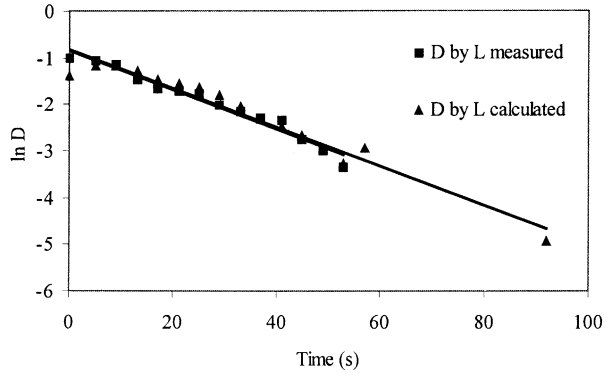

Fig. 5. Deformation D as a function of time for a PBT droplet immersed in an EMA matrix at 250 °C. Both curves obtained from L calculated and L measured were traced as well as their linear fit.

interfacial tension for the studied blend. From an experimental point of view, the real value of the major axis cannot be measured. Actually, the velocity gradient upon the gap generates an angle between the major axis of the ellipsoid and the shear direction. Hayashi et al. [12] demonstrate the dependence of this angle on the deformation imposed. However, the minor axis of the ellipsoid is not affected by this angle. Assuming that the deformed drop is a symmetrical ellipsoid and considering the volumes conservation, the major axis can be calculated from the following expression:

$$L = 8R_0^3/B^2 \quad (9)$$

When drawing on the same graphic, the time evolution of both the experimentally measured (without angle correction) major axis and the calculated one, we have noticed near values of the curves slope. Knowing that the major axis is far bigger than the minor one, the measurement accuracy will be better on the former. Consequently, the interfacial tension can be determined from the observed values of ellipsoid axis without angle correction.

As regards the EMA/PBT blend studied here, an average value of the interfacial tension has been calculated from the viscosities of the components (Table 1):

$$\gamma_{12}(\text{EMA/PBT})_{250\ ^\circ\text{C}} = 3.6\ \text{mN/m} \quad (10)$$

3. Results and discussion

In the experimental section, we have described the way to prepare the samples for optical shear experiments. In fact, the sample consists in a sandwich of two EMA films between which small particles of ground PBT are dispersed. The sandwich is placed between two quartz windows and the temperature is then increased to 250 °C, which is far above the melt temperature of PBT ($T_f^0 = 245\ ^\circ C$). A shear flow of 0.34 s^{-1} is applied for 3 min so as to deform the PBT particles. As discussed in Section 1, the dimensionless parameter Ca (Eq. (2)) controls the deformation of the drop sheared in a liquid matrix. The critical value of Ca can be calculated by the following expression from de Bruijn [13] as a function of the viscosity ratio p:

$$\log(\text{Ca}_{crit}) = -0.506 - 0.0994\log(p) + 0.124(\log(p))^2 - \frac{0.115}{\log(p) - 0.6107} \quad (11)$$

In our conditions, $\text{Ca}_{crit} \approx 0.485$.

From the size of the molten initial particles of PBT and the previously measured value of the interfacial tension of the EMA/PBT blend, knowing the viscosity of each components, we could give, according to Eq. (2), a couple of values between which the capillary number vary during

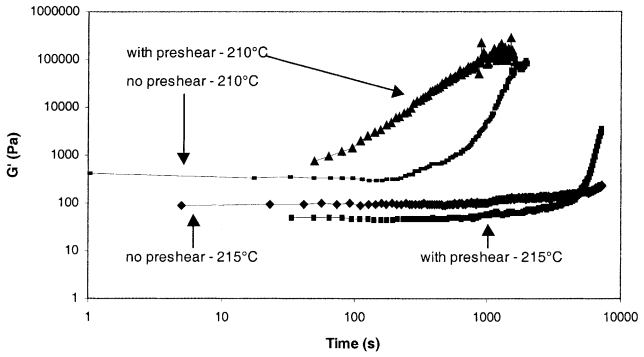

Fig. 6. Variation of the storage modulus versus time. Influence of a preshear treatment on the isothermal crystallization time of pure PBT at 210 and 215 °C.

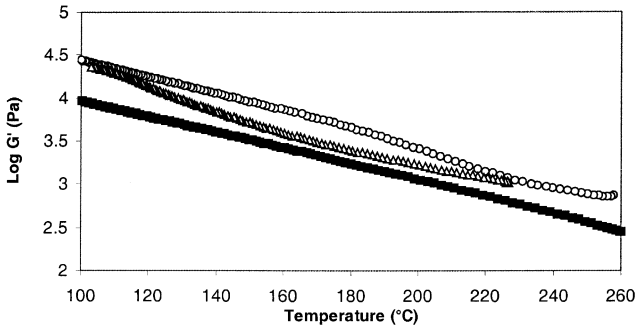

Fig. 7. Variation of the storage modulus versus temperature. Influence of preshear treatment on crystallization of PBT particles in EMA/PBT 70/30 blends. (■) EMA pure, (△) without preshear (○) preshear.

the shear treatment:

$$7.60 \leq \mathrm{Ca} \leq 22.81 \tag{12}$$

In this case, the values of Ca obtained are far above the critical value. The PBT particles actually turn into filaments as predicted by the literature. In fact, Janssen and Meijer [14] assumed that in shear flow, when $\mathrm{Ca} > 2\mathrm{Ca}_{\mathrm{crit}}$, initially affine stretching occurs and the droplets deform into filaments. Then, depending on the ratio $\mathrm{Ca}/\mathrm{Ca}_{\mathrm{crit}}$, the stretching becomes non-affine and next, after the droplet is deformed substantially, the deformation becomes affine again. Experiments have been carried out with different shear rates so as to select the optimal value of 0.34 s^{-1}. Actually, for smaller shear rates, the formation of fibers is a long process and thermal degradation becomes a major problem. On the contrary, for higher shear rates, the formation of fibers is very fast but substantial diameter reduction causes too many breaks of slender filaments. However, shear rates between 0.05 and 0.68 s^{-1} will be used to demonstrate the influence of shear rate on the crystallization of PBT fibers.

At the end of the 3 min shear treatment, we start studying the crystallization of the PBT dispersed in the EMA matrix. In this study, we have focused on the two main parameters: the crystallization time and the shear rate. In the first part, we focus the effects of crystallization on the relaxation of the fibers and consequently on the morphology development as a function of the crystallization time. Then we will deal with the influence of the shear flow during the crystallization process. However, we will first deal with a phenomenon that could accelerate the crystallization process. Indeed, Janeschitz-Kriegl et al. [15] demonstrates that shear treatment on molten polypropylene ones enhances its nucleation rate and therefore can reduce the crystallization time by two orders in magnitude. Kornfield et al. [16] attributes this phenomenon to the formation of an oriented structure induced by distortion of polymer chains. Although PBT chains are shorter than of polypropylene, a similar but attenuated behavior should be hoped for PBT. Boutahar et al. [17] demonstrates that during crystallization, transformed fraction is linked to the dynamic modulus. In this way, dynamic time sweep tests, using cone-plate geometry, were carried out at $\dot{\gamma} = 1\ s^{-1}$ on samples of pure PBT that have undergone, or not, a preshear treatment at 1 s^{-1} for 2 min. Substantial decrease could be observed on the crystallization time of shear induced crystallized PBT during isothermal treatment at both 210 and 215 °C (Fig. 6). On the other hand, in dispersed conditions, shear enhanced crystallization of PBT seems to be less effective depending on the process. During a rapid cooling process, a presheared blend of EMA/PBT 70/30 crystallizes between 220 and 190 °C. A non-presheared blend crystallizes between 160 and 115 °C (Fig. 7). In isothermal conditions, dispersed PBT does not crystallized, with or without preshear treatment, even at low isothermal temperatures ($T < 210$ °C). A corresponding experiment is carried out in differential scanning calorimetry (DSC) and leads to the same conclusion. Such observations were made by Pesneau et al. [18] on PE/PBT blend 80/20. Indeed, they suggested that molten PBT inclusions still exist at high supercooling. They also demonstrate that the crystallization rate does not increase with time at a fixed temperature. We will not go further in this subject since our work does not aim at understanding the origin of the enhancement of the crystallization growth rate or why dispersed PBT does not crystallize. These rheological experiments aim at evaluating the crystallization time of PBT in shear flow. In addition, it must be specified that blend samples for these tests were obtained from blend prepared with an internal mixer. As a consequence, the morphology of the blends used with the optical shear device is far coarser ($\phi \approx 100$ μm) than that used for the rheological tests ($\phi \approx 2$ μm) and consequently, the crystallization behavior of large PBT domains and finely dispersed PBT is hoped to be different.

3.1. Static crystallization

After the 3 min preshear, the shear is stopped as soon as the isothermal temperature is reached or as soon as the cooling ramp starts.

First of all, we carried out isothermal experiments in order to control the crystallization time. The latter can

Table 3
Experimental break-up times of molten fibers as a function of temperature and diameter

210 °C		215 °C		260 °C	
D_0 (μm)	t_b (s)	D_0 (μm)	t_b (s)	D_0 (μm)	t_b (s)
14.3	298	10.10	180	20.5	110
6.7	100	9.2	165	11.8	75
5	65	8.9	150	11	52
		8.4	135	9.8	36

considerably vary according to the cooling rate used or the isotherm temperature and as a consequence, the final morphologies could be very different. The simplest morphology obtained is a classical nodular one due to break-up of molten fibers before crystallization. Indeed, the break-up time of molten fibers must be taken into account. If the crystallization is too slow, the molten fiber is allowed to relax. Knowing that it has been generated, thanks to shear treatment with a Ca greater than the critical value, break-up of the fiber is expected. Testa et al. [19] has shown that for strong drop deformation, generating slender filaments, a sudden decrease in shear rate leads to break-up. Break-up times could be predicted from the work of Huneault et al. [20] and Elemans et al. [21] based on the theory of Tomotika [6]. Huneault et al. [20] gives the break-up time of molten fiber in quiescent state or submitted to a shear flow:

Break-up time in quiescent state:

$$t_b = \frac{2\eta_m R_0}{\gamma_{12}\Omega(\chi_m, p)} \ln\left(\frac{\alpha_r}{\alpha_i}\right) \quad (4)$$

Break-up time in shear flow:

$$t_b = \left[\frac{\eta_m \ln(\alpha_r/\alpha_i)}{\gamma_{12}\Omega(\chi_m, p)\dot{\gamma}^{1/2}} R_0\right]^{2/3} \quad (13)$$

with:

$$\alpha_i = \left(\frac{21kT}{8\pi^{3/2}\gamma_{12}}\right)^{1/2} \quad (14)$$

$$\alpha_r = 1.64R_0 \quad (15)$$

$\Omega(\chi_m, p)$ is the complex tabulated function of Tomotika [6]. α_i and α_r are the initial and break-up amplitude of the Rayleigh instability. D_0 represents the initial diameter of the thread, k the Boltzmann's constant and T the temperature. Experimental break-up times for various diameters of fibers and temperatures are presented in Table 3. Theoretical break-up times are presented in Table 4. As regards our work, we are in a transient case since the shear flow is stopped after 3 min and the generated molten fibers relax toward an equilibrium shape and then break-up by Rayleigh instabilities. This is the reason why experimental times measured are included between the theoretical break-up time in shear flow and in quiescent state. So despite the fact that there is an additional time due to relaxation of the molten fiber after shearing, the growing of the Rayleigh instabilities generated by the stop of flow makes the fiber break-up sooner. Nodular morphology has been obtained for two isotherm experiments, at 210 and 215 °C. Referring to the DSC analysis, we could predict the start of the crystallization after about 200 s at 210 °C and 1100 s at 215 °C. As a consequence, the increase in fiber viscosity, due to crystallization, will not slow down efficiently the relaxation process in time and thereby will not prevent the fiber from breaking. A nodular morphology is therefore expected. Regarding the crystallization times involved, a shear enhancement phenomenon following the fiber formation by shear flow should be negligible in this case. Such phenomenon is demonstrated in an isothermal experiment carried out at 209 °C. The rate of crystallization is too slow to stop the relaxation of the fiber by the crystallization process. The thinnest fibers having short relaxation times break into several drops. The biggest ones crystallized during the relaxation process and this leads to two types of structures. The former consists in fibers that have broken into smaller domains as they were partially crystallized. The latter consists in wavy fibers, the shape of which comes from Rayleigh instabilities that have been fixed by the excess in viscosity due to crystallization. The competition between relaxation of the molten PBT fibers and their crystallization are shown in Fig. 8.

From that point of view, fibrillar morphology should be obtained if the crystallization time is shorter than the break-up time. This is demonstrated in an isothermal experiment carried out at 206 °C. It leads to a mainly fibrillar morphology with a few broken pieces emerging from the relaxation of the smallest fibers. The morphological change that

Table 4
Theoretical break-up times of molten fibers as a function of temperature and diameter

210 °C			215 °C			260 °C		
D_0 (μm)	t_b (s) Quiescent	t_b (s) Shear	D_0 (μm)	t_b (s) Quiescent	t_b (s) Shear	D_0 (μm)	t_b (s) Quiescent	t_b (s) Shear
14.3	732.8	110.3	10.10	311	62	20.5	163	41
6.7	315.7	62.9	9.2	281	58	11.8	89	27
5	227.7	42.8	8.9	270	57	11	82	26
		50.6	8.4	253	55	9.8	72	24

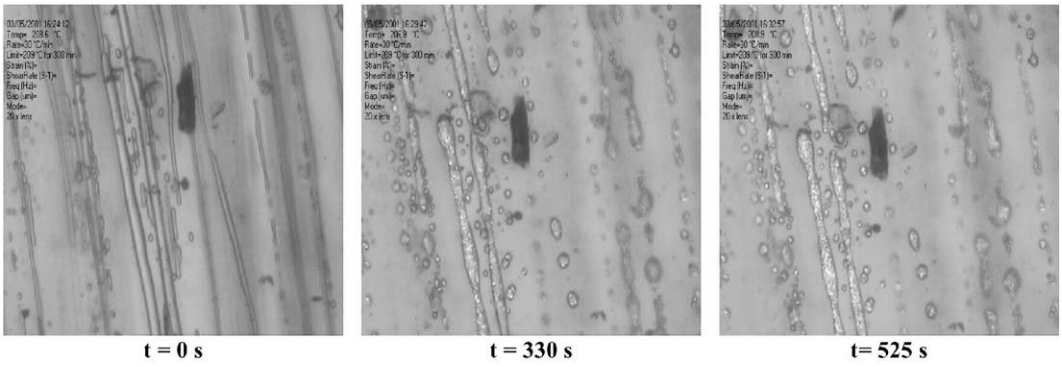

Fig. 8. Static crystallization of EMA/PBT blend at 209 °C; competition between relaxation of molten PBT fibers and their crystallization. The crystallized parts appear in white on the fibers.

occurred during this experiments are shown in Fig. 9. Note that the shear enhancement of crystallization of molten PBT fibers is quite important. Indeed, in Figs. 8 and 9, we can notice that crystallization is completed quite before the half time of crystallization measured in DSC. So as to reduce drastically the crystallization time, a controlled cooling ramp could be applied to the molten PBT fibers as soon as the shear flow is stopped. As the Linkam shear device enables such experiments, we have decided to carry out experiments at three different cooling rates: 2, 10 and 30 °C/min. Thanks to the DSC analysis, we could predict the crystallization onset temperatures at each cooling rate. At 2 °C/min, the crystallization onset temperature is about 201, 198 °C for 10 °C/min and 190 °C for 30 °C/min. For the two fastest cooling rates, the crystallization is so quick that the shear enhancement could be negligible. This assumption is justified since the experimental start temperatures are 206 °C at 2 °C/min, 198 °C at 10 °C/min and 190 °C at 30 °C/min. The shear effect on crystallization is only effective for long crystallization times. As shown in Fig. 10, decreasing drastically the crystallization time (or increasing the cooling rate from 10 to 30 °C/min) prevents the fibers in developing of Rayleigh instabilities. Thus, the PBT fibers that have been crystallized at 10 °C/min are slightly wavy whereas those crystallized at 30 °C/min are regular. The crystallization times involved during such experiments are far shorter (71 s at 10 °C/min and 42 s at 30 °C/min) than those observed for isothermal experiments. Regarding the experiment carried out at 2 °C/min, we could not say that the crystallization time is really reduced. On the contrary, nearly 2 min elapsed before the start of crystallization and the stop of shear flow. As a consequence, most of the thinnest fibers have already been broken by Rayleigh instabilities before the crystallization reaches a sufficient rate; notice that as soon as the crystallization starts, its growth rate is high, due to permanent temperature decrease, and the instabilities are stopped in a very short time. No further break-up of fibers is observed. Such phenomenon is pointed out on the first picture of Fig. 10. The so obtained morphology consists in the coexistence of more or less long wavy fibers and polymorphous particles; particles composed of nodules and deformed droplets crystallized during relaxation.

3.2. Dynamic crystallization

It consists in a continuous shear flow, even during the crystallization of the PBT fibers generated during the first 3 min of shear. As well as in the previous part, isothermal crystallization and controlled cooling crystallization have been studied. In order to take clear pictures during the

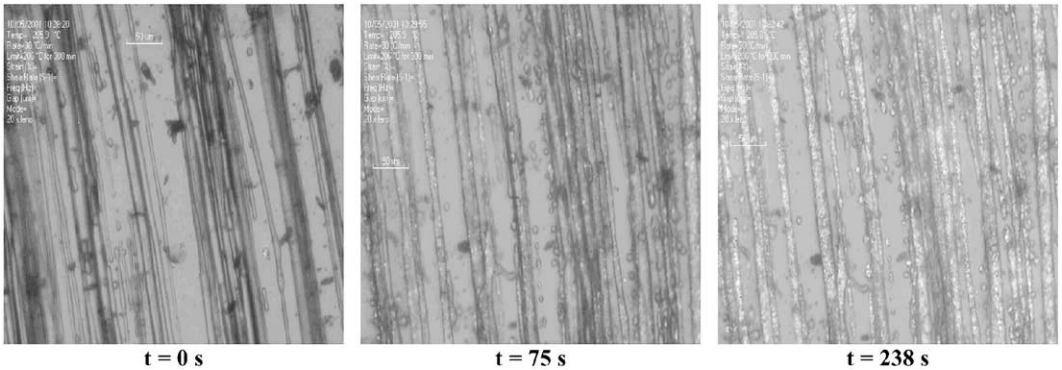

Fig. 9. Static crystallization of EMA/PBT blend; isothermal at 206 °C. The small white line on the pictures correspond to 50 μm.

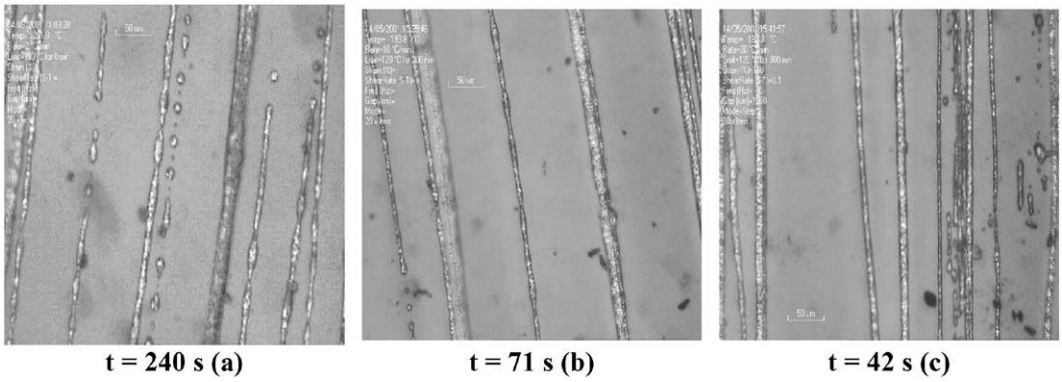

Fig. 10. Static crystallization of EMA/PBT blend; (a) cooling rate = 2 °C/min, (b) cooling rate = 10 °C/min, (c) cooling rate = 30 °C/min. The small white line on the pictures correspond to 50 μm.

dynamic cooling process experiments, we stop and resume the shear flow just for a few seconds.

As we have demonstrated in the previous part, the crystallization time has to be short enough so as to perpetuate the fibrillar morphology. During dynamic experiments, other parameters have to be taken into account, for instance, the heterogeneity development of the crystallization along the fiber under shear flow. Such phenomenon was also observed during static experiments and was responsible for the wavy shape of partially crystallized fibers. In dynamic experiments, the same effect appears and will be responsible for the premature breaking of partially crystallized fibers. Indeed, as the PBT crystallized, its viscosity increases drastically till it becomes infinite, when no more chain movements are possible. Consequently, there is a major viscosity difference between molten parts of the fiber and already crystallized parts. Undergoing the shear flow, molten parts will be able to deform whereas partially crystallized ones will not. Such breaking process is shown in Fig. 11. In these pictures, we can see that a molten part of the fiber, situated between two white crystallized parts, is able to deform. This process leads to fast diameter reduction of the molten areas that could eventually break-up. This explains the irregularities in fiber width as well as the flood of broken pieces observed at the end of the crystallization. Final morphologies obtained for isothermal at 206 and 210 °C are shown in Fig. 12. We can notice that decreasing the crystallization time limits the development of the irregularities along the fiber. Indeed, although the crystallization starts in a heterogeneous way along the fiber, the remaining molten parts

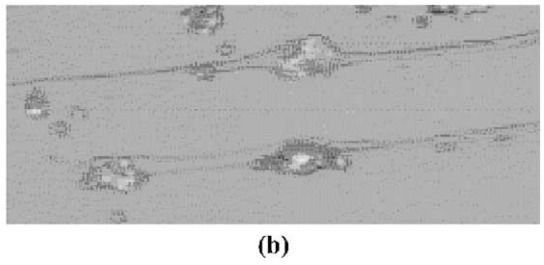

Fig. 11. Dynamic crystallization (a) isotherm at 206 °C, (b) isotherm at 210 °C; zoom on the irregularities' development on a PBT fiber, due to the heterogeneous crystallization along the fiber.

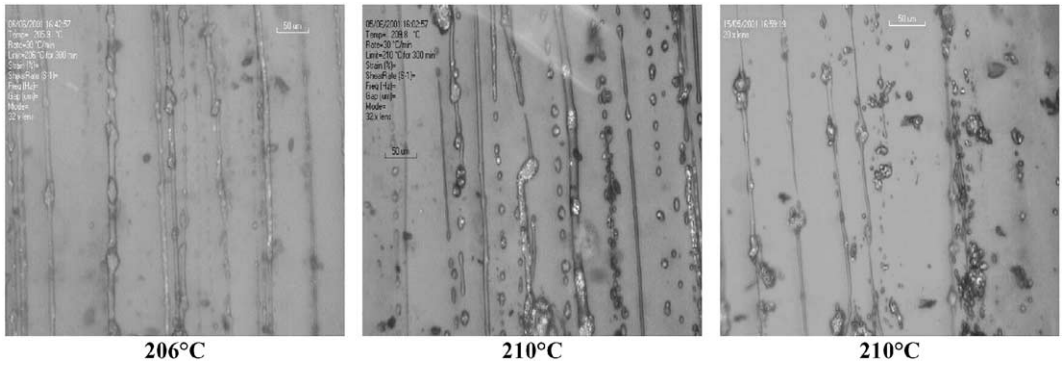

Fig. 12. Dynamic crystallization—isothermal experiments; breaking of PBT filaments due to heterogeneous crystallization along the fiber. The small white line on the pictures correspond to 50 μm.

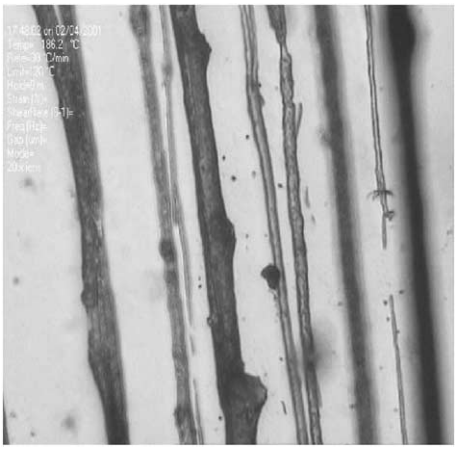

Fig. 13. PBT fibers crystallized during dynamic cooling at 0.34 s^{-1} with a cooling rate of 30 °C/min. The small black line on the pictures correspond to 50 μm.

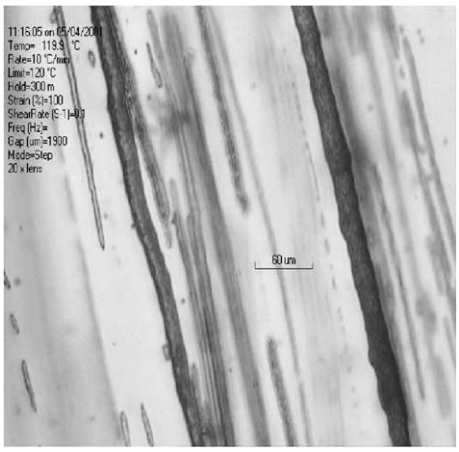

Fig. 15. PBT fibers crystallized during dynamic cooling at 0.17 s^{-1} with a cooling rate of 10 °C/min. The small black line on the pictures correspond to 60 μm.

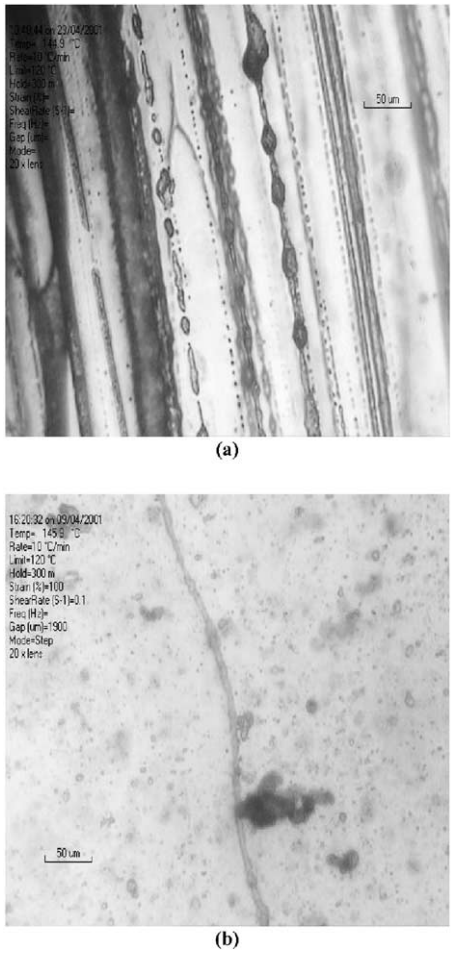

Fig. 14. PBT fibers crystallized during dynamic cooling at (a) 0.68 s^{-1} with a cooling rate of 10 °C/min and (b) 1.7 s^{-1} with a cooling rate of 2 °C/min. The small black line on the pictures correspond to 50 μm.

crystallize in a rather short time, which prevents the fiber from further deformation. This complex mechanism drives the morphology of the blend during the dynamic crystallization. Therefore, in order to keep the fibrillar morphology through the dynamic crystallization process, an instantaneous crystallization is required. Even by using the fastest cooling rate of the shear device, we could not reduce the crystallization time efficiently. Therefore it was not possible to obtain regular fibers with the dynamic crystallization process. Fig. 13 shows the final morphology of an EMA/PBT blend that has undergone a dynamic crystallization at 0.1 rad/s and a cooling rate of 30 °C/min. Even the remaining fibers are rather long, the adopted shape confirms our assumption about the heterogeneous development of the crystallization along the fiber.

In the dynamic cooling process, the crystallization time is an important parameter, however, the shear rate is another one. Indeed, so as to limit the effect of heterogeneous deformation along the fiber, we have to modify the shear rate. Actually, increasing the shear rate will lead to more break-up. Indeed the limited effect of shear enhancement crystallization time will not balance with the increase in deformation rate due to an increase in the shear rate. Experiments have been carried out to demonstrate that over a shear rate of 0.68 s^{-1} (Fig. 14), most of the fibers break during the crystallization and lead to a flood of small particles. Only the biggest filaments resist. As a matter of fact, decreasing the shear rate is the only solution to solve the problem of fiber breaking during the crystallization. Such experiment gives good results and is shown in Fig. 15.

4. Conclusions

The crystallization under shear flow of shear generated PBT fibers dispersed in an EMA matrix have been studied. The influence of crystallization time, break-up time of

filaments and shear rate on the final morphology of the blend has been demonstrated. The study was divided in two parts for comprehension purpose. First we focused on the static crystallization of the PBT filaments so as to understand the influence of crystallization time on morphology. We can deduce three headlines:

1. crystallization time $\gg$ break-up time = nodular morphology
2. crystallization time $\ll$ break-up time = fibrillar morphology
3. crystallization time $\approx$ break-up time = thin fibers lead to nodules and thick fibers adopt a more or less pronounced wavy shape.

Secondly we studied the dynamic crystallization and notably the breaking process of crystallizing fibers during shear flow and the influence of shear rate. We have brought to the fore that shear induced crystallization development is heterogeneous along the fibers and leads to the premature breaking of the fibers. Two solutions enable to keep fibrillar morphology. The former consists of a drastic reduction of the crystallization time by using a substantial cooling rate. The latter consists of a decrease of the shear rate during the crystallization so as to limit the deformation of partially crystallized fibers. Shear enhancement of the PBT crystallization was demonstrated as well, which favor the fibrillar morphology.

As a consequence of these experiments, we are able to control the morphology resulting from a dynamic crystallization. A nodular morphology can be obtained using long crystallization time. The nodule size can be controlled as well. High shear rates will lead to very small nodules. Low shear rates will result in coarser nodules. In order to keep a fibrillar morphology, short crystallization times are required, as well as low shear rates.

From the complex morphologies generated by crystallization under simple shear flow, we can expect very complex structures [7] resulting from extrusion or injection process.

Acknowledgements

Y.D. is grateful to the French Minister of research for providing him with a research assistantship. Thanks are also due to Dr J.P. Chapel for valuable discussions about the measurement of the interfacial tension of melt polymers.

References

[1] Taylor GI. Proc R Soc Lond, A 1934;146:501.
[2] Grace HP. Chem Engng Commun 1982;14:225.
[3] Bentley BJ, Leal LG. J Fluid Mech 1986;167:241–83.
[4] Acrivos A. Ann NY Acad Sci 1983;404:1–11.
[5] Rallison JM. Annu Rev Fluid Mech 1984;16:46–66.
[6] Tomotika S. Proc R Soc, A 1935;150:322–37.
[7] Cassagnau P, Michel A. Polymer 2001:3139–52.
[8] Luciani A, Champagne MF, Utracki LA. J Polym Sci, Polym Phys Ed 1997;35:1393.
[9] Sigillo I, di Santo L, Guido S, Grizzut N. Polym Engng Sci 1997;37:1540–9.
[10] Son Y, Yoon JT. Polymer 2001;42:7209–13.
[11] Xing P, Bousmina M, Rodrigue D. Macromolecules 2000;33:8020–34.
[12] Hayashi R, Takahashi M, Kajihara T, Yamane H. J Rheol 2001;45:627–39.
[13] R.A. de Bruijn. PhD thesis, Eindhoven University of Technology, 1989.
[14] Janssen JMH, Meijer HEH. J Rheol 1993;37:597–608.
[15] Janeschitz-Kriegl H, Eder G, Jerschow P. Int Polym Process 1993;VIII:3.
[16] Kornfield A, Kumaraswamy G, Issaian A. Macromolecules 1999;32:7537–47.
[17] Boutahar K, Carrot C, Guillet J. Macromolecules 1998;31:1921–9.
[18] Pesneau I, Cassagnau P, Fulchiron R, Michel A. J Polym Sci 1998;36:2573–85.
[19] Testa C, Sigillo I, Grizzuti N. Polymer 2001;42:5651–9.
[20] Huneault MA, Champagne MF, Luciani A. Polym Engng Sci 1996;36:1694–706.
[21] Elemans PHM, Janssen JMH, Meijer HEH. J Rheol 1990;34:1311–25.